

## Influence of Ordering in Porous TiO<sub>2</sub> Layers on Electron Diffusion

Shay Tirosch,<sup>†</sup> Thomas Dittrich,<sup>\*,‡</sup> Ashi Ofir,<sup>†</sup> Larisa Grinis,<sup>†</sup> and Arie Zaban<sup>\*,†</sup>

Chemistry Department, Bar-Ilan University, Ramat-Gan, 52900, Israel, and  
Hahn-Meitner-Institute, Glienicke Str. 100, D-14109 Berlin, Germany

Received: June 9, 2006; In Final Form: July 13, 2006

Layers of porous TiO<sub>2</sub> fabricated by electrophoretic deposition at different temperatures with subsequent sintering in air were investigated by transient photocurrent measurements in aqueous electrolyte. The effective diffusion coefficient of excess electrons changed between  $1.6 \times 10^{-5}$  and  $1.4 \times 10^{-4}$  cm<sup>2</sup>/s depending strongly on the solution temperature during the TiO<sub>2</sub> layer deposition. Characterization, in terms of average degree of preferred orientation, shows that low deposition temperature results in orientation of the nanocrystals forming the porous film. Consequently, the increase of effective diffusion coefficient is attributed to a higher degree of ordering in the nanoporous TiO<sub>2</sub> layer.

### Introduction

Local ordering is crucial for electronic transport in porous networks of interconnected nanoparticles. Ordering in porous networks can be associated with geometrical aspects such as coordination number of the nanocrystals forming the network<sup>1,2</sup> or preferential orientation of the nanocrystals with respect to the network axes. Figure 1 provides a schematic illustration of increasing orientation of nanocrystals in a network, from the *random* case (Figure 1c) to *perfect orientation* of monodispersed nanocrystals (Figure 1a). *Partial orientation* like the one shown in Figure 1b may be realized by application of electric fields during the deposition of the nanocrystals from electrolyte solutions.<sup>3,4</sup>

Recently, we developed an electrophoresis based deposition method that enables fabrication of high quality reproducible porous TiO<sub>2</sub> layers for application in dye-sensitized solar cells.<sup>5</sup> In this work we utilized the electrophoretic deposition (EPD) method to fabricate nanoporous TiO<sub>2</sub> electrodes with different levels of orientation. This is achieved by a control of the deposition temperature based on the understanding that the electric field induced orientation needs to counter the thermal motion of the particles during the deposition. Characterization, in terms of the average degree of preferred orientation (expressed as texture coefficient), shows a gradual intensification of the nanocrystals orientation with decreasing deposition temperature.

Electron transport in porous TiO<sub>2</sub> layers can be described by the effective diffusion coefficient ( $D_{\text{eff}}$ ),<sup>6,7</sup> which is measured by photocurrent transients excited in porous electrodes immersed in electrolyte. Typical values for  $D_{\text{eff}}$  are on the order of  $10^{-5}$  cm<sup>2</sup>/s.<sup>6</sup> In this work, it is demonstrated that  $D_{\text{eff}}$  can be changed up to 1 order of magnitude by ordering of the nanocrystallites in the porous TiO<sub>2</sub> layer whereas the porosity and the recombination parameters remain unchanged.

### Experimental Section

**(a) Electrode Preparation.** Porous TiO<sub>2</sub> layers were fabricated by constant current electrophoretic deposition (EPD) on conducting glass substrates (SnO<sub>2</sub>:F, Pilkington) from a suspension containing the TiO<sub>2</sub> nanocrystals (P-25, Degussa). Details of the deposition technique are reported elsewhere.<sup>5</sup> The layer thickness ( $L$ ), controlled by the deposition duration, was determined by a DECTAC step-profiler.

A series of nanoporous TiO<sub>2</sub> electrodes of different thicknesses (1.8–13 μm) were prepared at room temperature to evaluate the correlation between the thickness ( $L$ ) and the effective diffusion coefficient ( $D_{\text{eff}}$ ). A second series consisting of nanoporous TiO<sub>2</sub> electrodes of practically similar thicknesses was fabricated while the temperature of the nanocrystals suspension was varied during the EPD process ( $T_{\text{EPD}}$ ). The temperature range, –25 to +65 °C was expected to affect the order in the porous film; thus the second series was used to investigate the influence of ordering on  $D_{\text{eff}}$ .

**(b) Measurement of the Electrode Porosity.** The porosity was determined via measurements of surface-to-volume ratio in the electrodes. The TiO<sub>2</sub> surface area was determined by dye adsorption. The nanoporous TiO<sub>2</sub> layers were immersed overnight in a  $3 \times 10^{-4}$  M ethanol solution of the N3 dye (Ru-[(2,2'-bipyridine-4,4'-(COOH)<sub>2</sub>]<sub>2</sub>(NCS)<sub>2</sub>). To determine the amount of adsorbed dye molecules, the electrodes were dipped in a 1 M NaOH solution followed by spectral measurements of the dye concentration in the solution. The electrodes surface areas were calculated using a value of 1.65 nm<sup>2</sup> occupied by a dye molecule.<sup>8</sup> The film thickness was measured with a profilometer.

The surface area to film volume ratios of the films prepared at different deposition temperatures were practically similar. In other words, the porosity and thus the coordination number of nanoparticles in the films reported here were not affected by the deposition temperature.

**(c) Orientation Analysis of the Porous TiO<sub>2</sub> Layers by X-ray Diffraction.** X-ray diffraction (XRD) patterns were used

\* Corresponding author. E-mail: A.Z., zaban@mail.biu.ac.il.

<sup>†</sup> Bar-Ilan University.

<sup>‡</sup> Hahn-Meitner-Institute.

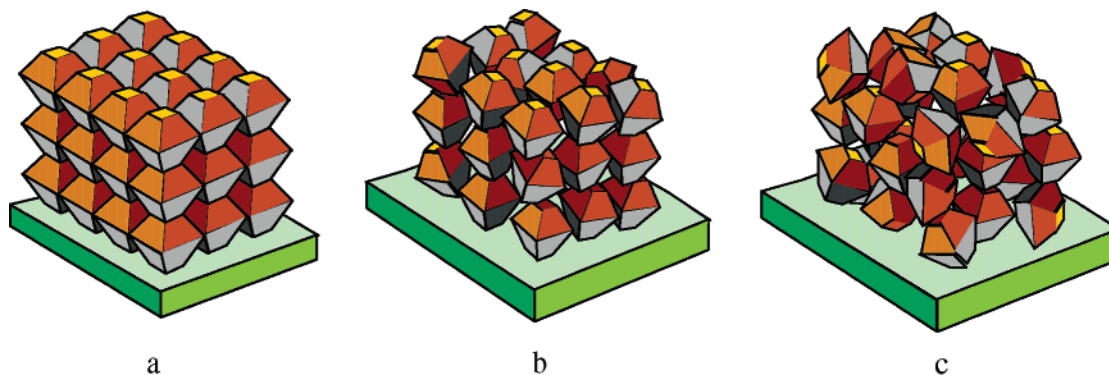


**Figure 1.** Anatase TiO<sub>2</sub> nanoparticles with their truncated polygon crystal habit, packed in three main possibilities in a nanoporous layer: (a) perfectly oriented nanoparticles; (b) partially oriented nanoparticles; (c) randomly oriented nanoparticles.

to determine the grain size variations, phase fractions and the average degree of preferred orientation (ADPO) in the nanoporous TiO<sub>2</sub> films. XRD patterns were recorded in  $2\theta$  configuration using an X-ray diffractometer (Rigaku 2028) with Cu K $\alpha$  radiation (40 kV and 40 mA), Ni filter, receiving slit 0.2 mm and divergence slit 1°. All samples were scanned between 20° and 56° at a step size of 0.02° and scan rate of 2.5°/s. The grain size variations of the anatase and the rutile fractions were determined from the peak broadening at  $\langle 200 \rangle$  and  $\langle 110 \rangle$  reflections, respectively. In this study the peak broadening is solely related to the grain size. This approach is supported by the fact that the grain size calculated from XRD without stress consideration (25 nm) is similar to the size observed in the TEM micrographs.

The TiO<sub>2</sub> phase fractions of anatase and rutile and the ADPO were analyzed according to the Reitveld refining method using the EXPGUI software.<sup>9,10</sup> The refinement was based on a three phase model with anatase, rutile and cassiterite (SnO<sub>2</sub> layer on the glass substrate). The SnO<sub>2</sub> layer has an orientation in axis  $[0\bar{2}0]$  with a March–Dollase strength of  $r = 0.45688$ . For the refinement, a preferred orientation (PO) profile correction that takes into account the March–Dollase formulation<sup>11</sup> assuming multicompeting preferred orientation was used. The preferred orientations for  $\langle 101 \rangle$ ,  $\langle 004 \rangle$ ,  $\langle 200 \rangle$ ,  $\langle 112 \rangle$ ,  $\langle 103 \rangle$ , and  $\langle 211 \rangle$  of anatase reflections and  $\langle 110 \rangle$  and  $\langle 101 \rangle$  of rutile reflections were introduced into the refining model. For simplicity the ADPO calculation focused on an orientation direction that is perpendicular to the scattering vector of any  $\langle h,k,l \rangle$  reflection. ADPO is then reduced to the simple form given by

$$\text{ADPO} = \frac{1}{\sum_{i=1}^N \chi_i r_i^{3/2}} \quad (1)$$

where  $\chi_i$  and  $r_i$  are the refined volume fractions and the refined preferred orientation strengths of  $N$  examined reflections that result from the refinement process. We note that the best fitting was achieved in the Reitveld refinement, after application of the profile correction of March–Dollase.

The fraction of anatase amounted to  $0.78 \pm 0.04$  in all porous TiO<sub>2</sub> layers, independent of EPD treatment. This result corresponds well with the reported value of P25.<sup>12</sup> Further, there were no changes in the grain sizes or in the size distributions of both the anatase and the rutile nanoparticles upon variation of EPD treatment.

**(d) Photocurrent Transient Measurements.** Photocurrent (PC) transients were measured on porous TiO<sub>2</sub> electrodes immersed in 0.5 M NaCl (pH = 2.5) electrolyte. The PC transients were excited with pulses of the third harmonic of a Nd:YAG laser (wavelength 355 nm, duration time of a laser

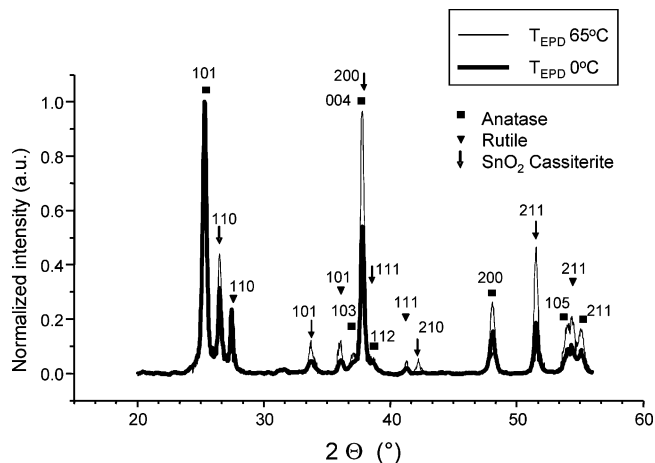


**Figure 2.** XRD profiles of films prepared using EPD under 0 and 65 °C.

pulse 150 ps, intensity up to  $W = 0.9 \text{ mJ/cm}^2$ , EKSP312) and detected with a CompuScope 14200-128M. The effective diffusion coefficient ( $D_{\text{eff}}$ ) was obtained from the PC transients using the following equation:<sup>6</sup>

$$D_{\text{eff}} = \frac{L^2}{6t_{\text{peak}}} \quad (2)$$

where  $t_{\text{peak}}$  is the time at which the maximum of the PC transient is reached and  $L$  is the thickness of the nanoporous TiO<sub>2</sub> film which is not illuminated by the light pulse.

The repetition rate of the laser pulses was 10 Hz. The times of the characteristic peaks of the PC transients are much shorter than 100 ms, and the system relaxes within this time as well (example shown in Figure 4).

## Results and Discussion

### (a) Ordering in Porous TiO<sub>2</sub> Layers Induced by EPD.

Figure 2 shows two representative normalized XRD diffractograms obtained for  $T_{\text{EPD}} = 65$  and 0 °C ( $T_{\text{EPD}}$  represents the temperature of the nanocrystals suspension during the EPD process). The normalization refers to the main peak intensity of the  $\langle 101 \rangle$  anatase reflection. The characteristic reflections of the anatase TiO<sub>2</sub>, rutile TiO<sub>2</sub> and cassiterite SnO<sub>2</sub> (the transparent conductive substrate) phases are indicated. There are clear differences between the two spectra (compare, for example, the intensities of the  $\langle 200 \rangle$  and  $\langle 211 \rangle$  reflections of the two diffractograms). Generally, out of the two diffractograms, the XRD pattern of the  $T_{\text{EPD}} = 65$  °C case is closer to that of random

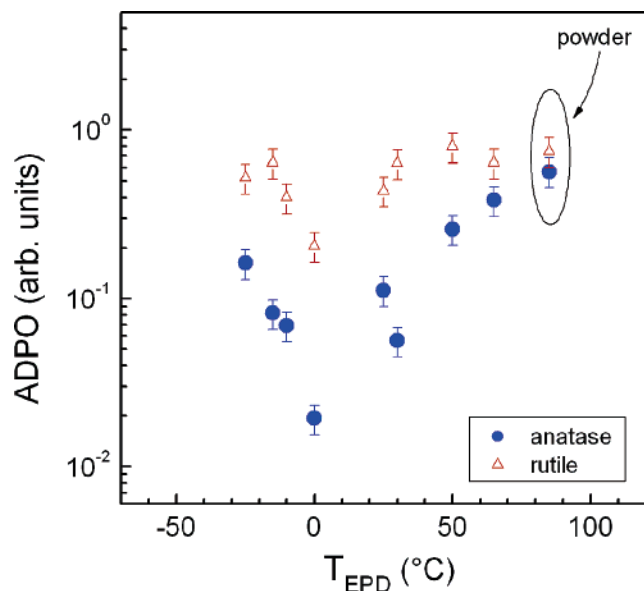


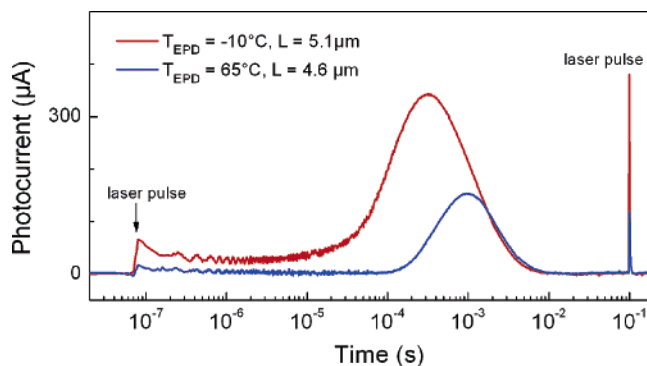
**Figure 3.** Average degree of preferred orientation (ADPO) of anatase and rutile in nanoporous films dependent on their EPD preparation temperature.

powder. However, information about ordering can be obtained only after detailed refinement analysis.

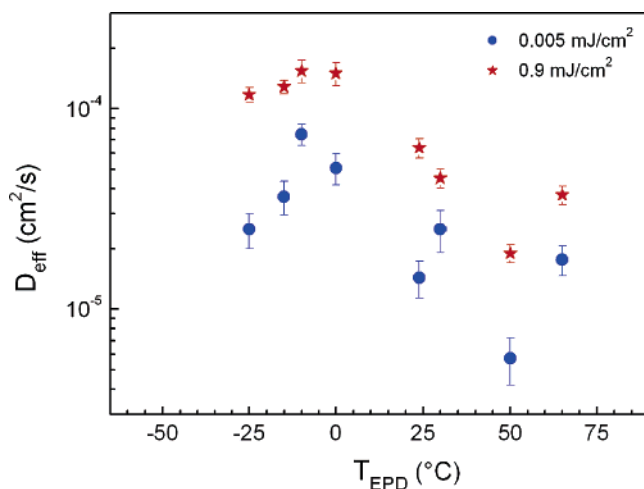
Diffraction profile refinement using March–Dollase corrections was carried out for all porous TiO<sub>2</sub> series. Fitting quality and the crystallographic weighting Reitveld parameters rang within  $2.34 < \chi^2 < 4.73$  and  $0.053 < R_{wp} < 0.634$ , respectively. The quality of the refinement is not ideal due the complexity of the system; however, refinement with no orientation or with only one orientation direction gave much worse fitting quality. Therefore, the ADPO presented here should be regarded only as the main tendency of EPD induced ordering in the nanoporous TiO<sub>2</sub> films

Figure 3 shows the ADPO values of the anatase and rutile nanocrystals in the porous TiO<sub>2</sub> layers as a function of  $T_{EPD}$ . For comparison, the ADPO values of P25 powder (the randomly oriented reference), are presented in Figure 3. The ADPO of the P25 powder amounts to about 0.57 for the anatase crystals and 0.8 for the rutile fraction of the powder. The general trend associated with the EPD process is a decrease of ADPO values compared with those of the random powder, i.e., introduction of ordering on the nanocrystallites with respect to the glass substrate. Even at  $T_{EPD} = 65$  °C the ADPO values are smaller than those of the random powder (0.36 for anatase and 0.62 for rutile). The minimum ADPO values, observed around  $T_{EPD} = 0$  °C for both anatase and rutile, indicate that the degree of ordering is maximal at this deposition temperature. We note, however, that the minimum ADPO values are quite different for the anatase and the rutile fractions of the films, 0.02 and 0.2, respectively. This means that the ordering induced by the EPD is much more pronounced for anatase than for the rutile nanoparticles. We believe that this effect is related to differences in the polarizability of anatase and rutile nanocrystallites.

Figure 3 further shows that the tendency to form higher ordering with decreasing deposition temperature inverses at 0 °C. The values of ADPO increased with decreasing  $T_{EPD}$  below 0 °C, indicating lower degree of ordering. This observation contradicts the thermal activation approach that connects orientation with slower Brownian motion of the nanocrystals at lower  $T_{EPD}$ . Therefore, it seems that at deposition below 0 °C parameters other than the Brownian motion become dominant. The effect is currently studied by suggesting several



**Figure 4.** Photocurrent transients profiles of transients passed through nanoporous films prepared by EPD under  $-10$  and  $+65$  °C. (Transients executed using a laser excitation energy of  $0.9$  mJ/cm<sup>2</sup>.)



**Figure 5.** Temperature dependent on the effective diffusion coefficient calculated from transients that were excited using laser energy of  $0.005$  mJ/cm<sup>2</sup> (circles) and  $0.9$  mJ/cm<sup>2</sup> (stars).

options such as water condensation into the deposition suspension or local temperature induced changes of either the pH or the ionic strength. These physical changes seem to influence the surface and thus the polarizability of the nanocrystals. Results will be published when conclusive.

#### (b) Determination of the Effective Diffusion Coefficient.

PC transients of several porous TiO<sub>2</sub> layers of different thicknesses were measured. The peaks of the photocurrent transients shift systematically to shorter times with decreasing layer thickness as expected for diffusion controlled transport. The values of  $t_{peak}$  were measured for different intensities of the laser pulses ( $W$ ) and analyzed using eq 2. The values of the effective diffusion coefficients ( $D_{eff}$ ) change between  $4 \times 10^{-6}$  cm<sup>2</sup>/s ( $L = 4.2$  µm,  $W = 2$  µJ/cm<sup>2</sup>) and  $4 \times 10^{-5}$  cm<sup>2</sup>/s ( $L = 10.5$  µm,  $W = 0.9$  mJ/cm<sup>2</sup>).  $D_{eff}$  increases with increasing  $W$  tending toward saturation at the higher pulse intensities where it becomes independent of  $L$ . Such a behavior is well-known in the literature.<sup>2</sup>

#### (c) Influence of Ordering in the Porous TiO<sub>2</sub> Layers on $D_{eff}$ .

PC transients of porous TiO<sub>2</sub> layers prepared at different  $T_{EPD}$  were investigated at room temperature for  $W = 0.44$  and  $0.9$  mJ/cm<sup>2</sup>. At these intensities  $D_{eff}$  is almost saturated. Figure 4 presents PC transients of two porous TiO<sub>2</sub> layers prepared at  $T_{EPD} = -10$  and  $+65$  °C. The thicknesses of the two layers were quite similar, i.e.,  $L = 5.1$  and  $4.6$  µm for  $T_{EPD} = -10$  and  $+65$  °C, respectively. However,  $t_{peak}$  of the layer deposited at  $65$  °C is reached at much longer times compared with that for the layer deposited at  $-10$  °C. This means that  $D_{eff}$  of the

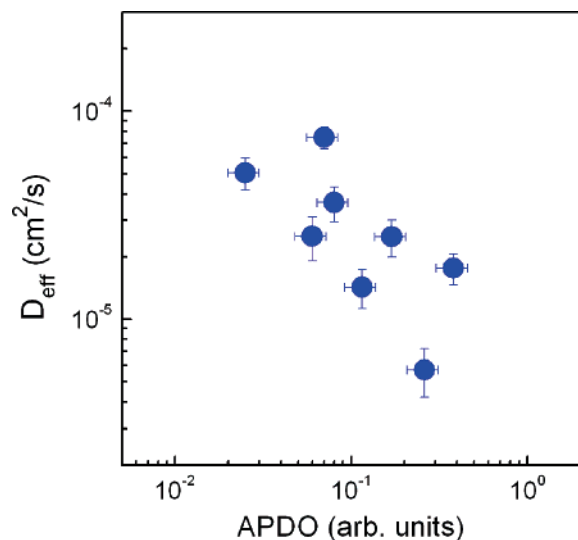


**Figure 6.** Effective diffusion coefficient dependent on the average degree of preferred orientation (ADPO) in anatase nanoparticles (transients executed using laser excitation energy of 0.9 mJ/cm<sup>2</sup>).

porous TiO<sub>2</sub> layer deposited at +65 °C is much smaller than  $D_{\text{eff}}$  of the layer deposited at −10 °C.

Figure 5 shows the dependence of  $D_{\text{eff}}$  on  $T_{\text{EPD}}$  at two illumination intensities. The highest values of  $D_{\text{eff}}$ ,  $\sim 1.4 \times 10^{-4}$  cm<sup>2</sup>/s, were observed in films deposited at  $T_{\text{EPD}}$  between −10 and 0 °C. Film deposition at  $T_{\text{EPD}} < -10$  °C results in a small decrease of  $D_{\text{eff}}$  to about  $1 \times 10^{-4}$  cm<sup>2</sup>/s whereas an increase of  $T_{\text{EPD}}$  above 0 °C, results in an order of magnitude decrease of  $D_{\text{eff}}$  to about  $1.7 \times 10^{-5}$  cm<sup>2</sup>/s ( $T_{\text{EPD}} = 50$  °C). The charge integrated over a PC transient was practically independent of  $T_{\text{EPD}}$  ( $L$  was nearly constant in these experiments). This shows that the recombination rate of the photo-generated electrons with the electrolyte present in the porous electrode is not influenced by  $T_{\text{EPD}}$  or by the induced preferential orientation. We note in this respect that in previous experiments of this type it was shown that the integrated charge is strongly influenced by surface defect concentration.<sup>13</sup> Consequently, the deposition temperature and the resulting ordering do not modify the surface defect.

Figure 6 integrates the results presented in Figures 3 and 5 showing the preferential orientation of the nanocrystallites

(smaller ADPO) strongly increases the effective diffusion coefficient in porous TiO<sub>2</sub> layers.

### Summary

Ordering of nanocrystallites in porous TiO<sub>2</sub> layers was obtained using electrophoretic deposition in a wide temperature range. The origin of the ordering and differences between ordering of the anatase and the rutile structured nanocrystallites are not well understood yet. The highest degree of ordering, expressed as the lowest ADPO value, correlated with the highest values of effective diffusion coefficient measured in these films. The results should lead to improvement of photoelectrochemical application like dye-sensitized solar cells. Moreover, our experiments open new opportunities for fundamental investigations related to percolation in porous networks and to the role of relative nanocrystal orientation on transport in related systems.

**Acknowledgment.** We are grateful to Dr. S. Dube and Dr. S. Bönišch (HMI) for installing a system for the measurement of logarithmic transients. The BIU group acknowledges the financial support provided by the Israel Science Foundation founded by The Israel Academy of Science and Humanities. S.T. acknowledges the support of the Israeli ministry of science, The Eshcol scholarship.

### References and Notes

- (1) Benkstein, K. D.; Kopidakis, N.; van-de Lagemaat, J.; Frank, A. J. *J. Phys. Chem. B* **2003**, *107*, 7759.
- (2) Frank, A. J.; Kopidakis, N.; van-de Lagemaat, J. *Coord. Chem. Rev.* **2004**, *248*, 1165.
- (3) Schwan, H. P.; Sher, L. D. *J. Electrochem. Soc.* **1969**, *116*, 22C.
- (4) Muth, V. E. *Kolloid. Z.* **1927**, *41*, 97.
- (5) Dittrich, T.; Ofir, A.; Grinis, L.; Tirosh, S.; Zaban, A. *Appl. Phys. Lett.* **2006**, *88*, 182110.
- (6) Solbrand, A.; Lindstrom, H.; Rensmo, H.; Hagfeldt, A.; Lindquist, S.-E.; Sodergren, S. *J. Phys. Chem. B* **1997**, *101*, 2514.
- (7) Soedergren, S.; Hagfeldt, A.; Olsson, J.; Lindquist, S. E. *J. Phys. Chem.* **1994**, *98*, 5552.
- (8) Halme, J. *Department of Engineering Physics and Mathematics*; Helsinki University of Technology: Helsinki, 2002; p 115.
- (9) Toby, B. H. *J. Appl. Crystallogr.* **2001**, *34*, 210.
- (10) Larson, A. C.; Von Dreele R. B. Los Alamos National Laboratory, Los Alamos, 2000, LAUR 86.
- (11) Dollase, W. A. *J. Appl. Crystallogr.* **1986**, *19*, 267.
- (12) de-Almedia, P.; Van-deelen, J.; Catry, C.; Sneyers, H.; Pataki, T.; Andriessen, R.; van-Roost, C.; Kroon, J. M. *Appl. Phys. A* **2004**, *79*, 1819.
- (13) Ruhle, S.; Dittrich, T. *J. Phys. Chem. B* **2006**, *110*, 3883.